Composite Vortex Manipulation as a Design Tool for Reflective Intelligent Surfaces

Mirko Barbuto , *Senior Member, IEEE*, Andrea Alù , *Fellow, IEEE*, Filiberto Bilotti , *Fellow, IEEE*, and Alessandro Toscano , *Senior Member, IEEE*

Abstract—To achieve a smart electromagnetic (EM) environment, several implementation challenges need to be addressed. Among them, the practical realization of low-cost and easily deployable reconfigurable intelligent surfaces (RISs) is a crucial objective for both the applied EM and wireless communication communities. In this framework, we propose a new design strategy for adding reconfigurability to reflective metasurfaces (MTSs) and, thus, implementing RISs. In particular, we exploit the insights of CV theory to control the overall scattering pattern of reflective MTSs and reduce the complexity of the control system. Indeed, instead of continuously tuning the response of each MTS element, the proposed solution requires only switching on and off the response of a portion of the MTS itself, allowing for an easier practical implementation. The results of an analytical analysis and a set of numerical full-wave simulations confirm the effectiveness of the proposed approach.

Index Terms—Composite vortex, metasurfaces, reconfigurability, reflective intelligent surfaces, smart electromagnetic (EM) environment.

I. INTRODUCTION

RECONFIGURABLE intelligent surfaces (RISs) have been recognized as a key enabling technology for beyond 5G wireless systems [1], [2], [3]. This kind of planar structure typically consists of scattering elements, whose electromagnetic (EM) response can be independently controlled to achieve the desired overall scattering pattern when excited by an external EM field. In this way, by properly covering them with RISs, the objects in the environment can be transformed from mere obstacles for signal propagation to actual relays or transceivers with an active role in the reliability and capacity of the communication channel [4]. Although this approach provides a number of degrees of freedom, it also involves several implementation challenges [5], [6]. In particular, a proper deployment strategy

Mirko Barbuto is with the Department of Engineering, "Niccolò Cusano" University, 00166 Rome, Italy (e-mail: mirko.barbuto@unicusano.it).

Andrea Alù is with the Advanced Science Research Center, City University of New York, New York, NY 10017 USA (e-mail: alu@mail.utexas.edu).

Filiberto Bilotti and Alessandro Toscano are with the Department of Industrial, Electronic, and Mechanical Engineering, ROMA TRE University, 00154 Rome, Italy (e-mail: filiberto.bilotti@uniroma3.it; alessandro.toscano@uniroma3.it).

should be implemented for maximizing channel performance while, at the same time, taking into account several practical factors, such as the deployment cost, the user distribution, the available space, and the propagation conditions. In addition, the possibility of tailoring the EM response of the object typically involves the use of large RISs. Therefore, an efficient design strategy for minimizing the complexity of the RISs should be implemented.

In this framework, a crucial role is played by metasurfaces (MTSs) that, being constituted by electrically small and subwavelength-spaced passive elements [7], [8], [9], allow for a fine tuning of the EM response and a low-cost implementation. Still, we need to independently control the response of each element of the MTS, resulting in significant complexity in the case of large structures. Indeed, the massive use of active components (e.g., varactor diodes, MEMS, etc.) and the large number of control lines, limit the large-scale deployment of RISs.

In the literature, some interesting solutions to simplify the design and implementation of reconfigurable MTSs have been proposed [10], [11], [12], [13], [14]. In particular, the concept of digital MTS allows to control the EM field using different coding sequences, which can be pre-evaluated, stored, and switched in real time using a field programmable gate array (FPGA) [11]. Still, the external control circuit typically needs to evaluate a huge number of coding sequences and actively control all the MTS elements independently. Another interesting approach consists of mutually twisting two closely stacked MTSs [14]. In this way, one can synthesize far-field scattering patterns through the direct contact of mutually twisted fully passive metallic patterns. However, this requires a mechanic rotating system, which is not compatible with the extreme low-latency required by beyond-5G wireless systems.

In this letter, we propose a new mechanism for reaching dynamic tuning of RISs through the composite vortex (CV) theory. Indeed, instead of controlling the response of each individual element of a MTS, we concentrically placed two circular MTSs that, when excited by an impinging plane wave, produce different vortex modes. The superimposed vortex beams give rise to an overall scattering pattern, which varies as a function of the relative amplitude and phase of excitation of the two modes. A similar approach has been recently proposed for tuning the radiation pattern of patch antennas [16], [17]. However, here, the vortex modes are not excited at the source level, but rather generated after reflection from an illuminated properly structured MTS. In addition, the proposed approach is not limited to the generation of different vortex modes for multiplexing applications [18], [19], [20], [21], [22], [23], but it is exploited in the context of CV theory in order to give design
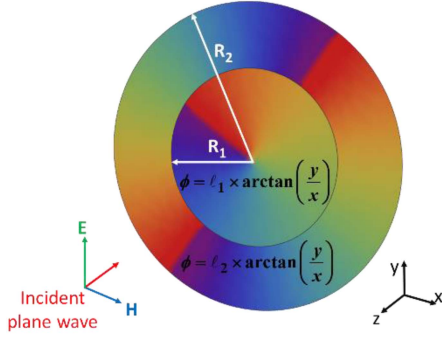
Fig. 1. Sketch of a circular reflective MTS divided into an inner circular disk surrounded by an external ring, which imparts a different helical phase profile to a vertically polarized orthogonal impinging plane wave (as an example, the colors represent the phase response for: $\ell_1 = 1$, $\ell_2 = 2$, $\delta = \pi/2$).

guidelines for RISs, whose response can be tailored in a much simpler way.

We remark here that some preliminary results on this topic have been discussed in our recent conference paper [15] which, however, was limited to a pure analytical analysis. In this letter, in addition to providing more details on the analytical results, we also propose a practical implementation based on a realistic model and full-wave simulations.

II. PROBLEM FORMULATION AND ANALYTICAL RESULTS

Vortex modes belong to a specific class of EM fields exhibiting a hollow intensity distribution due to a phase singularity point [24]. To expand their potential, they can be combined together to form the so-called *composite vortices* [25]. Indeed, the overall field distribution, in both amplitude and phase, can be finely manipulated by properly balancing the constituting beams. This phenomenon has been successfully employed to design a wide range of practical devices [26], [27], [28], [16], [17]. A similar approach is exploited here to manipulate the scattering pattern of a reflective MTS and, thus, simplify the reconfigurable strategies of RISs.

For this purpose, we start our analysis by considering that a single reflective MTS can be designed to impart a helical phase profile $e^{j\ell\varphi}$ and, thus, transform an impinging plane wave into a reflected vortex mode [19], [20], [21], [22], [23], [29], [30]. Ideally, the MTS should exhibit a reflection of unitary amplitude and a phase response

$$\phi = \ell \times \arctan\left(\frac{y}{x}\right) \tag{1}$$

where ℓ is the vortex order mode and we have assumed a metasurface placed in the xy-plane.

In our case, we need to superimpose two different vortex modes. Thus, the considered reflective MTS, reported in Fig. 1, consists of two regions, i.e., an inner circular disk surrounded by an external ring, each one exhibiting a reflection of unit amplitude but a helical phase profile of different order (ℓ_1 and

ℓ_2, respectively). In this case, the overall scattering pattern can be written as [21] where $_1F_2$ is the hypergeometric function, R_1 and R_2 are the radii of the inner and outer region of the MTS, respectively, δ is the added phase shift between the two modes, and θ and ϕ represent the elevation and azimuth angles, respectively.

Equation (2) shown at the bottom of this page can be directly used to compute the response of the overall MTS, once the main geometrical and EM parameters are fixed. However, due to the presence of the hypergeometric functions, it does not allow for a simple analysis of the problem and for implementing a clear design strategy. On the contrary, several physical insights can be inferred directly from the CV theory. Indeed, the analysis reported in [25] demonstrated that, by properly choosing the order of the constituting vortex beams (i.e., ℓ_1 and ℓ_2), the number of phase singularity points and, thus, of amplitude nulls, can be chosen at will. In addition, the positions of these nulls can be manipulated by simply acting on the relative amplitude and phase of the two modes, further increasing the possibilities for reconfiguring the MTS response. Therefore, depending on the requirements for a specific application, the overall MTS can be designed to reflect the desired composite vortices and, thus, exhibit the required number of amplitude nulls.

Here, we focus our attention in the simplest case of the superposition of a vortex-free component ($\ell_1 = 0$) and a vortex mode of the first order ($\ell_2 = 1$). In this case, we have seen that the overall field still exhibits a phase singularity point, whose position depends on the amplitude and phase of the vortex-free component [16]. Specifically, by increasing the amplitude of the vortex-free component, the distance from the center of the singularity point can be increased, while by acting on the relative excitation phase, the singularity point can be rotated on the azimuthal direction. These two knobs, i.e., the relative amplitude and phase of the two modes, can be, thus, exploited for controlling the scattering pattern of the overall MTS.

To demonstrate the effectiveness of this new design strategy, we have first analyzed the scattering pattern (2) for the specific case of interest (i.e., $\ell_1 = 0$ and $\ell_2 = 1$), once the electrical dimension of the external ring $R_2 = 1.5\,\lambda_0$ is fixed. In this case, as shown in Fig. 2, the overall scattering pattern can be controlled by acting on R_1 (i.e., the radius of the central region exhibiting a constant phase shift). Indeed, by increasing the radius of the inner part, we increase the vortex-free component of the overall field and, thus, we move away the radiation null from the original central position [16]. In this way, also the shape of the scattering pattern can be tailored between the conical one, when the whole MTS reflects a vortex mode of the first order (i.e., $R_1 = 0$), and the broadside one when the whole MTS reflects a vortex-free component (i.e., $R_1 = R_2$). Indeed, between these two limiting cases, we can tilt the reflected beam in the angular range $\theta < 15°$. Moreover, Fig. 3 shows the three-dimensional (3D) scattering patterns for different values of the phase shift δ between the two constituting regions, once fixed $R_1 = \lambda_0$. In this case, the scattering pattern can be also rotated along its center, allowing for a 2-D beam scanning [16].

$$|F_{tot}(\theta, \varphi)| = \sqrt{1 - (\sin\varphi\sin\theta)^2} \left| \sum_{n=1}^{2} \frac{(-jk\sin\theta)^{|\ell_n|} e^{j\ell_n\varphi + j(n-1)\delta}}{2^{|\ell_n|}\,|\ell_n|!\,(|\ell_n| + 2)} \left[R_n^{|\ell_n|+2}\,{}_1F_2\left(\theta, |\ell_n|, R_n\right) - R_{n-1}^{|\ell_n|+2}\,{}_1F_2\left(\theta, |\ell_n|, R_{n-1}\right) \right] \right| \tag{2}$$
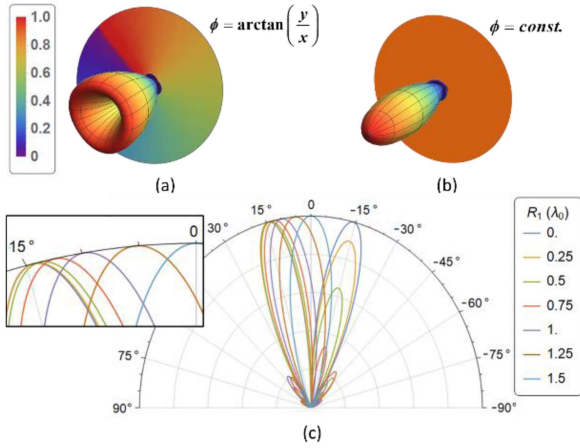
Fig. 2. 3-D normalized scattering patterns for the two limiting cases: (a) $R_1 = 0$ and (b) $R_1 = R_2 = 1.5\,\lambda_0$; (c) Normalized scattering pattern in the plane $\phi = \pi/2$ for different values of R_1 (here $\ell_1 = 0$, $\ell_2 = 1$), with a zoom on the main beam.
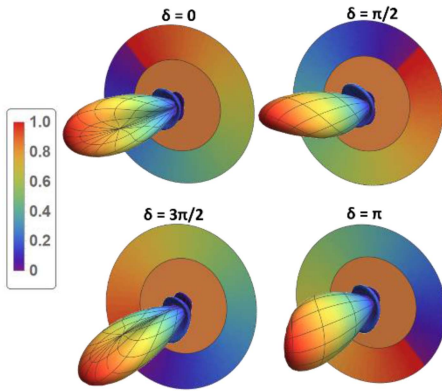

Fig. 3. 3-D normalized scattering patterns for different values of the phase shift δ between the two regions (here $R_1 = \lambda_0$, $R_2 = 1.5\lambda_0$, $\ell_1 = 0$ and $\ell_2 = 1$).

Please note that, in order to tailor the shape or the tilting angle of the reflected beam, here we just need to control the surface area ratio between the inner and outer MTS regions. Thus, compared to the standard design approach that is based on finely tuning the phase response of all the MTS elements by properly integrating tuning elements (e.g., varactor diodes), here we just need to "switch-OFF" the helical phase response of some of the MTS elements. Moreover, we remark here that, for the sake of brevity, we focused our attention to a specific configuration of composite vortices and a fixed dimension of the overall MTS, which give rise to specific reconfiguration capabilities (e.g., a main beam in the angular region $|\theta| < 15°$) of possible interest for indoor environments. However, the actual potentialities of this approach are not limited to this scenario, and, by properly choosing the overall dimension of the RIS and the order of the two modes, further manipulation capabilities can be implemented [17], [18]. In particular, for achieving a single beam with an increased maximum tilting angle, we need to increase the order of the external vortex mode ℓ_2, and chose the order of the inner region such that $\ell_1 = \ell_2 - 1$. In this way, the overall beam exhibits a central phase singularity of order ℓ_1-1, and a single (ℓ_2-$\ell_1 = 1$) external vortex, which can be moved to control the maximum tilting angle of the overall beam, as shown in Fig. 4.
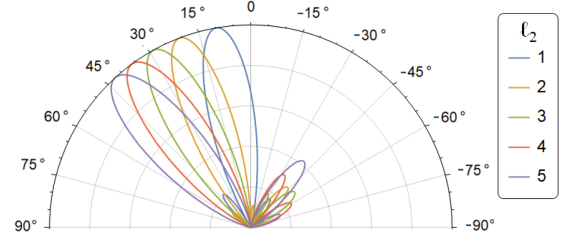

Fig. 4. 3-D normalized scattering patterns for different values of the higher order mode: here $\ell 1 = \ell 2$–1, R1 = λ, R2 = 1.5 λ.
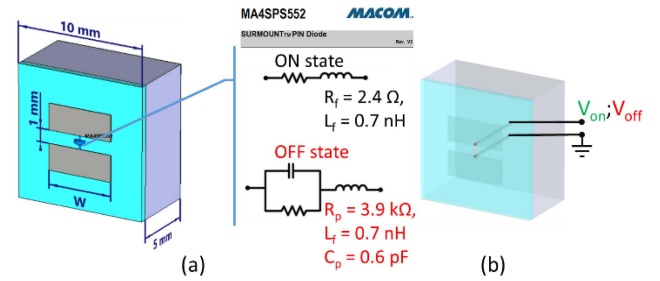

Fig. 5. (a) Perspective view of the proposed MTS element loaded with a PIN diode, which was modeled by the corresponding equivalent circuits for the ON and OFF states; (b) picture in transparency showing the biasing vias.

III. EXAMPLE OF A PRACTICAL IMPLEMENTATION

In the previous section, we have shown how the insights of CV theory can be directly exploited for tailoring the scattering pattern of RISs. For this purpose, we have considered ideal MTS sheets able to perfectly impart the required phase profile to the impinging field. However, for a practical realization, a realistic MTS with a finite number of elements should be implemented. Moreover, for a vortex mode of order ℓ, the MTS structure can be further simplified and divided into N equiangular sectors (being $|\ell| < N/2$), each one constituted by identical elements [29]. For this task, several successful examples have been proposed in the literature [21], [23], [29], [30]. In these cases, a reflective unit-cell with a full phase coverage (360°) and a unitary reflection amplitude have been designed. In addition, in our case we also need to switch-OFF the helical phase response for the inner part of the MTS and, thus, a reconfigurable strategy should be implemented. However, here, we do not need to continuously change the phase response of the unit-cell, but we only need to obtain an almost constant phase shift when the phase response is switched-off.

A possible solution for this goal is reported in Fig. 5 and consists of a squared metallic patch printed on a F4B dielectric substrate with thickness of 0.508 mm and relative permittivity $\varepsilon_r = 2.25$. This structure is spaced from a metallic sheet through a 5 mm thick foam layer. Moreover, the metallic patch, whose dimension w can be changed to achieve different phase shifts, has been cut at its center and loaded with a commercial PIN diode (MA4SP552 [31]). Finally, two metallic vias are embedded within the structure for setting the polarization voltages to the ON or OFF states of the diodes [32]. It is worth noticing that the thin biasing lines are orthogonal to the MTS plane and, thus, the effect on the unit-cell response is almost negligible. In addition, bringing the control lines beyond the ground plane, allow to isolate the MTS element from the control network that could be realized on the back of the overall MTS.
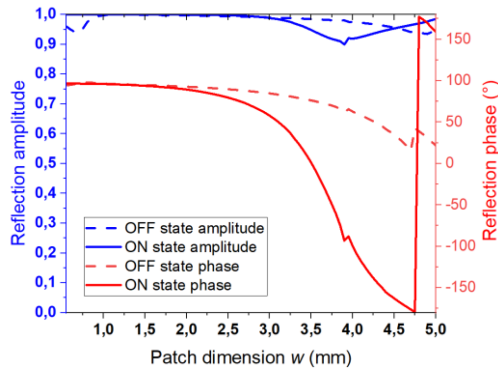
Fig. 6. Reflection amplitude and phase of the MTS element shown in Fig. 4 for different patch dimension w at 3 GHz.
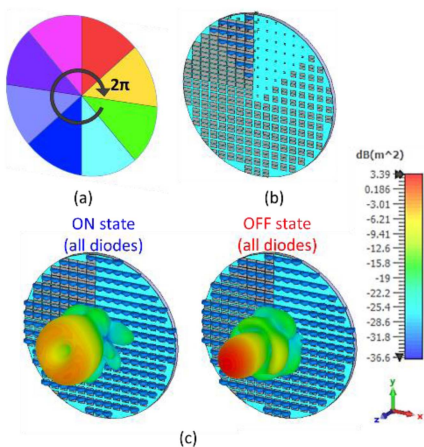

Fig. 7. (a) Geometrical representation of the eight sectors in which the MTS is divided for achieving the helical phase profile; (b) Eight-sector reflective MTS implemented by using the unit-cell reported in Fig. 4 (for better clarity of the image, the PIN diodes are shown for a sector only, but each element of the MTS is actually loaded); (c) 3-D scattering patterns for the two limiting cases: (left) all diodes are in their ON state, (right) all diodes are in their OFF state.

The unit-cell analysis has been performed by exploiting the equivalent circuit model of the PIN diode working at ON and OFF state [31] (shown in Fig. 5), and the corresponding results are reported in Fig. 6. This figure shows the amplitude and phase response of the unit-cell at 3 GHz and for different values of the patch dimension w. As expected, when the diode is in the ON state, i.e., the two elements of the patch are short-circuited, the proposed element is able to cover any phase value with a good reflection amplitude (greater than 0.9). On the contrary, when the diode is switched-OFF, the phase coverage is extremely reduced, still reflecting with an almost unitary amplitude, confirming the very low losses introduces by the PIN diodes.

This behavior can be thus exploited to design a realistic MTS, whose response can be controlled according to the analysis of the previous section. Indeed, as shown in Fig. 7, we have implemented a circular reflective MTS with radius $R_2 = 1.5\,\lambda_0$ and consisting of eight sectors [29], whose elements have been chosen according to (1) and considering $\ell_1 = 1$ and an ON state for all the diodes. In this case, when the diodes are actually on their ON state, the impinging plane wave is transformed into a reflected vortex mode with a scattering null at its center, as
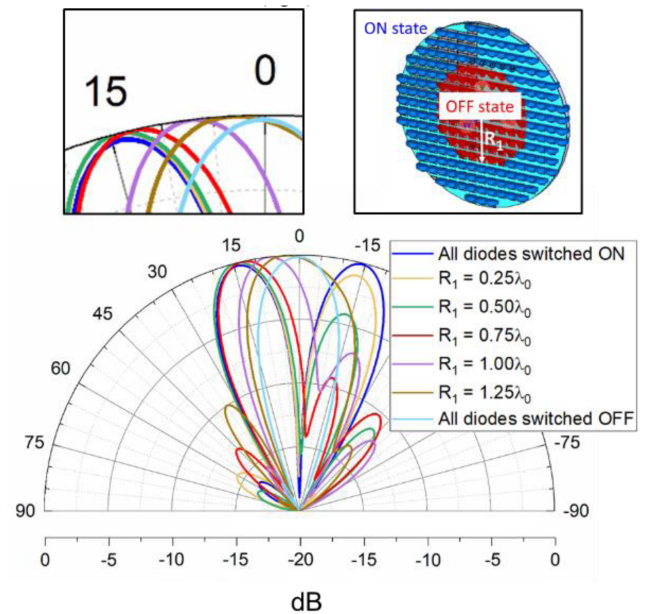

Fig. 8. Normalized scattering patterns in the plane $\phi = \pi/2$ for different values of R_1 (here $\ell_1 = 0$, $\ell_2 = 1$). In the inset: (left) zoom on the main beam direction; (right) the eight-sector reflective MTS where the PIN diodes falling in a region of radius R_1 are switched-OFF.

shown in Fig. 7(c). Instead, when all the diodes of the same MTS are switched-OFF, the impinging plane wave is reflected with an almost constant phase shift and, thus, a retro-reflective scattering beam is achieved. In between these two limiting cases, we can also switch-OFF simultaneously only a portion of the PIN diodes contained in a central circular region of radius R_1 and, thus, control the response of the MTS as analytically predicted in the previous section. Indeed, the scattering patterns reported in Fig. 8 (for different radii of the inner region where the diodes are switched-OFF) are coherent with the ones reported in Fig. 2, confirming our expectations.

Please note that some discrepancies exist in the main beam direction of the ideal and realistic cases that, however, could be reduced by implementing a finer tuning of the reflective MTS. In particular, in the realistic case, we are not able to switch-OFF a perfect circular region but we are limited by the finite dimensions of the unit-cell and their square shape. Finally, we remark here that the overall RIS exhibits good performance in terms of side-lobe level (lower than -7.5 dB) and polarization purity (cross-pol component lower than -30 dB).

IV. CONCLUSION

In this letter, we have proposed a possible solution to simplify the reconfigurability of reflective MTSs. In particular, by reporting both analytical and numerical results, we have shown that the scattering response of a reflective MTS can be controlled by exploiting the CV theory and, thus, reducing the number of control elements to only the relative amplitude and phase between the superimposed vortex components. This approach, although reducing the degrees of freedom compared to more consolidated approaches, allows for a simpler design and realization strategy, with a direct impact on the implementation of RISs in a smart EM environment.

REFERENCES

[1] M. Di Renzo et al., "Smart radio environments empowered by reconfigurable intelligent surfaces: How it works, state of research, and the road ahead," *IEEE J. Sel. Areas Commun.*, vol. 38, no. 11, pp. 2450–2525, Nov. 2020, doi: 10.1109/JSAC.2020.3007211.

[2] Y. Liu et al., "Reconfigurable intelligent surfaces: Principles and opportunities," *IEEE Commun. Surv. Tut.*, vol. 23, no. 3, pp. 1546–1577, Jul/Sep. 2021, doi: 10.1109/COMST.2021.3077737.

[3] Q. Cheng et al., "Reconfigurable intelligent surfaces: Simplified-architecture transmitters–from theory to implementations," *Proc. IEEE*, vol. 110, no. 9, pp. 1266–1289, Sep. 2022, doi: 10.1109/JPROC.2022.3170498.

[4] M. D. Renzo, F. H. Danufane, and S. Tretyakov, "Communication models for reconfigurable intelligent surfaces: From surface electromagnetics to wireless networks optimization," *Proc. IEEE*, vol. 110, no. 9, pp. 1164–1209, Sep. 2022, doi: 10.1109/JPROC.2022.3195536.

[5] X. Yuan, Y. -J. A. Zhang, Y. Shi, W. Yan, and H. Liu, "Reconfigurable-intelligent-surface empowered wireless communications: Challenges and opportunities," *IEEE Wireless Commun.*, vol. 28, no. 2, pp. 136–143, Apr. 2021, doi: 10.1109/MWC.001.2000256.

[6] R. Flamini et al., "Towards a heterogeneous smart electromagnetic environment for millimeter-wave communications: An industrial viewpoint," *IEEE Trans. Antennas Propag.*, vol. 70, no. 10, pp. 8898–8910, Oct. 2022, doi: 10.1109/TAP.2022.3151978.

[7] A. Díaz-Rubio, S. Kosulnikov, and S. A. Tretyakov, "On the integration of reconfigurable intelligent surfaces in real-world environments: A convenient approach for estimation reflection and transmission," *IEEE Antennas Propag. Mag.*, vol. 64, no. 4, pp. 85–95, Aug. 2022, doi: 10.1109/MAP.2022.3169396.

[8] M. Barbuto et al., "Metasurfaces 3.0: A new paradigm for enabling smart electromagnetic environments," *IEEE Trans. Antennas Propag.*, vol. 70, no. 10, pp. 8883–8897, Oct. 2022, doi: 10.1109/TAP.2021.3130153.

[9] G. Oliveri, F. Zardi, P. Rocca, M. Salucci, and A. Massa, "Building a smart EM environment - AI-enhanced aperiodic micro-scale design of passive EM skins," *IEEE Trans. Antennas Propag.*, vol. 70, no. 10, pp. 8757–8770, Oct. 2022, doi: 10.1109/TAP.2022.3151354.

[10] C. Della Giovampaola and N. Engheta, "Digital metamaterials," *Nature Mater.*, vol. 13, no. 12, pp. 1115–1121, Dec. 2014, doi: 10.1038/nmat4082.

[11] T. J. Cui, M. Q. Qi, X. Wan, J. Zhao, and Q. Cheng, "Coding metamaterials digital metamaterials and programmable metamaterials," *Light, Sci. Appl.*, vol. 3, Oct. 2014, Art. no. e218, doi: 10.1038/lsa.2014.99.

[12] T. J. Cui, S. Liu, and L. Zhang, "Information metamaterials and metasurfaces," *J. Mater. Chem. C*, vol. 5, pp. 3644–3668, 2017, doi: 10.1039/C7TC00548B.

[13] X. Fang, M. Li, D. Ding, F. Bilotti, and R. Chen, "Design of in-phase and quadrature two paths space-time-modulated metasurfaces," *IEEE Trans. Antennas Propag.*, vol. 70, no. 7, pp. 5563–5573, Jul. 2022, doi: 10.1109/TAP.2022.3145480.

[14] S. Liu, S. Ma, and T. J. Cui, "Moiré metasurfaces for dynamic beamforming," *Sci. Adv.*, vol. 8, no. 33, Aug. 2022, Art. no. eabo1511, doi: 10.1126/sciadv.abo1511.

[15] M. Barbuto, A. Alù, F. Bilotti, and A. Toscano, "Designing reflective intelligent surfaces through the composite vortex theory," in *Proc. 16th Int. Congr. Artif. Mater. Novel Wave Phenomena (Metamaterials)*, 2022, pp. X–052–X–054, doi: 10.1109/Metamaterials54993.2022.9920887.

[16] M. Barbuto, M.-A. Miri, A. Alu, F. Bilotti, and A. Toscano, "Exploiting the topological robustness of composite vortices in radiation systems," *Prog. Electromagn. Res.*, vol. 162, pp. 39–50, 2018, doi: 10.2528/PIER18033006.

[17] M. Barbuto, M.-A. Miri, A. Alù, F. Bilotti, and A. Toscano, "A topological design tool for the synthesis of antenna radiation patterns," *IEEE Trans. Antennas Propag.*, vol. 68, no. 3, pp. 1851–1859, Mar. 2020, doi: 10.1109/TAP.2019.2944533.

[18] M. Barbuto, A. Alù, F. Bilotti, and A. Toscano, "Dual-circularly polarized topological patch antenna with pattern diversity," *IEEE Access*, vol. 9, pp. 48769–48776, 2021, doi: 10.1109/ACCESS.2021.3068792.

[19] P. Genevet et al., "Ultra-thin plasmonic optical vortex plate based on phase discontinuities," *Appl. Phys. Lett.*, vol. 100, no. 1, Jan. 2012, Art. no. 013101, doi: 10.1063/1.3673334.

[20] F. Bouchard, I. De Leon, S. A. Schulz, J. Upham, E. Karimi, and R. W. Boyd, "Optical spin-to-orbital angular momentum conversion in ultra-thin metasurfaces with arbitrary topological charges," *Appl. Phys. Lett.*, vol. 105, no. 10, 2014, Art. no. 101905, doi: 10.1063/1.4895620.

[21] B. You, L. Zhou, L.-S. Wu, Y.-P. Zhang, and J.-F. Mao, "Theory of reflective phase-shifting surface for generating vortex radio waves," *IEEE Trans. Antennas Propag.*, vol. 64, no. 11, pp. 4942–4948, Nov. 2016, doi: 10.1109/TAP.2016.2602371.

[22] S. Yu, L. Li, and N. Kou, "Generation reception and separation of mixed-state orbital angular momentum vortex beams using metasurfaces," *Opt. Mater. Exp.*, vol. 7, no. 9, pp. 3312–3321, Sep. 2017, doi: 10.1364/OME.7.003312.

[23] L.-J. Yang, S. Sun, and W. E. I. Sha, "Ultrawideband reflection-type metasurface for generating integer and fractional orbital angular momentum," *IEEE Trans. Antennas Propag.*, vol. 68, no. 3, pp. 2166–2175, Mar. 2020, doi: 10.1109/TAP.2019.2948711.

[24] M. S. Soskin, V. N. Gorshkov, M. V. Vasnetsov, J. T. Malos, and N. R. Heckenberg, "Topological charge and angular momentum of light beams carrying optical vortices," *Phys. Rev. A*, vol. 56, pp. 4064–4075, 1997, doi: 10.1103/PhysRevA.56.4064.

[25] E. J. Galvez, N. Smiley, and N. Fernandes, "Composite optical vortices formed by collinear Laguerre-Gauss beams," *Proc. SPIE Nanomanipulation Light*, vol. 11, Art. no. 613105, Feb. 2006, doi: 10.1117/12.646074.

[26] D. G. Grier, "A revolution in optical manipulation," *Nature*, vol. 424, pp. 810–816, 2003, doi: 10.1038/nature01935.

[27] J. H. Lee, G. Foo, E. G. Johnson, and G. A. Swartzlander, "Experimental verification of an optical vortex coronagraph," *Phys. Rev. Lett.*, vol. 97, 2006, Art. no. 053901, doi: 10.1103/PhysRevLett.97.053901.

[28] T. Bauer et al., "Observation of optical polarization möbius strips," *Science*, vol. 347, pp. 964–966, 2015, doi: 10.1126/science.1260635.

[29] Z. Chang, B. You, L.-S. Wu, M. Tang, Y.-P. Zhang, and J.-F. Mao, "A reconfigurable graphene reflectarray for generation of vortex THz waves," *IEEE Antennas Wireless Propag. Lett.*, vol. 15, pp. 1537–1540, 2016, doi: 10.1109/LAWP.2016.2519545.

[30] H.-F. Huang and S.-N. Li, "High-Efficiency planar reflectarray with small-size for OAM generation at microwave range," *IEEE Antennas Wireless Propag. Lett.*, vol. 18, no. 3, pp. 432–436, Mar. 2019, doi: 10.1109/LAWP.2019.2893321.

[31] [Online]. Available: https://cdn.macom.com/datasheets/MA4SPS552.pdf

[32] J. Han, L. Li, G. Liu, Z. Wu, and Y. Shi, "A wideband 1 bit 12 × 12 reconfigurable beam-scanning reflectarray: Design, fabrication, and measurement," *IEEE Antennas Wireless Propag. Lett.*, vol. 18, no. 6, pp. 1268–1272, Jun. 2019, doi: 10.1109/LAWP.2019.2914399.